



## Research paper

# Chlorine dioxide inhibits the replication of porcine reproductive and respiratory syndrome virus by blocking viral attachment

Zhenbang Zhu, Yang Guo, Piao Yu, Xiaoying Wang, Xiaoxiao Zhang, Wenjuan Dong, Xiaohong Liu, Chunhe Guo\*

State Key Laboratory of Biocontrol, School of Life Sciences, Sun Yat-sen University, North Third Road, Guangzhou Higher Education Mega Center, Guangzhou, Guangdong 510006, PR China



## ARTICLE INFO

**Keywords:**  
PRRSV  
Chlorine dioxide  
Antiviral activity

## ABSTRACT

Porcine reproductive and respiratory syndrome virus (PRRSV) causes a great economic loss to the swine industry globally. Current prevention and treatment measures are not effective to control the outbreak and spread of porcine reproductive and respiratory syndrome (PRRS). In other words, new antiviral strategies are urgently needed. Chlorine dioxide (ClO<sub>2</sub>) is regarded as a broad-spectrum disinfectant with strong inhibitory effects on microbes and parasites. The purpose of this study was to evaluate the inhibitory effects and underlying molecular mechanisms of ClO<sub>2</sub> against PRRSV infection in vitro. Here, we identified ClO<sub>2</sub> (the purity is 99%) could inhibit the infection and replication of PRRSV in both Marc-145 cells and porcine alveolar macrophages (PAMs). ClO<sub>2</sub> could block PRRSV binding to cells rather than internalization and release, suggesting that ClO<sub>2</sub> blocks the first stage of the virus life cycle. We also demonstrated that the inhibition exerted by ClO<sub>2</sub> was attributed to the degradation of PRRSV genome and proteins. Moreover, we confirmed that ClO<sub>2</sub> could decrease the expression of inflammatory cytokines induced by PRRSV. In summary, ClO<sub>2</sub> is an efficient agent and potently suppressed PRRSV infection in vitro.

## 1. Introduction

Porcine reproductive and respiratory syndrome virus (PRRSV) is one of the most important pathogens that severely impacts swine industry worldwide (Yun and Lee, 2013). Porcine reproductive and respiratory syndrome (PRRS), caused by PRRSV, is an acute viral infectious disease. PRRS is characterized by reproductive failure in pregnant sows and respiratory diseases in pigs of all ages, which causes huge economic losses every year (Gomez-Laguna et al., 2013; Lunney et al., 2010). PRRSV is a member of the genus *Porartevirus* of the family *Arteriviridae* of the order *Nidovirales*, PRRS-1 (type 1 or European PRRSV) and PRRS-2 (type 2 or American PRRSV) are the two species in this genus (Guo et al., 2018; King et al., 2018). It is an enveloped, single-stranded, positive-sense RNA virus, which has an approximately 15 kb genome encoding at least 11 open reading frames (ORF). ORF1a and ORF1b accounting for about 75% of the full-length genome encode the non-structural proteins (NSP), which mainly act as RNA replicase and RNA polymerase (Fang and Snijder, 2010; Li et al., 2015); ORF2a, ORF2b, ORF3 and ORF4 encode the membrane glycoprotein GP2, GP3 and GP4, which are the secondary structural proteins of virus; ORF5, ORF6 and ORF7 encode glycoprotein GP5, matrix protein M and the

nucleocapsid protein N, respectively, which are relevant to viral entry and immunogenicity (Doan and Dokland, 2003; Dokland, 2010; Sarah K. Wootton et al., 1998; Yang et al., 2013; Zhang and Yoo, 2015). PRRSV can cause immunosuppression and induce persistent infection which has resulted in the difficulty of prevention and control of the disease (Kimmerman et al., 2009). Previous studies have reported that many natural compounds, microRNAs and new vaccinations can control PRRSV infection (Du et al., 2017a; Du et al., 2017b; Liu et al., 2017; Vu et al., 2017). However, there is limited protection against PRRSV infection even though current vaccination strategies were widely used. Therefore, developing a safe and effective antiviral strategy is needed.

Chlorine dioxide (ClO<sub>2</sub>) is a strong oxidizing agent with a broad range of biological activity against bacteria, virus, fungi and parasites (Sigstam et al., 2014). ClO<sub>2</sub> has more effective disinfection potential and produces fewer harmful by-products than other chloride (Dodd, 2012). ClO<sub>2</sub> is regarded as a potent and suitable disinfectant widely used in recent years. Many studies have certified that several viruses were inactivated effectively by the chlorination of ClO<sub>2</sub>, including human rotavirus (HRV) (Chen and Vaughn, 1990), human norovirus (HNoV) (Lim et al., 2010; Montazeri et al., 2017), feline calicivirus (FCV) (Montazeri et al., 2017), enterovirus71 (EV71) (Jin et al., 2013),

\* Corresponding author.

E-mail addresses: [liuxh8@mail.sysu.edu.cn](mailto:liuxh8@mail.sysu.edu.cn) (X. Liu), [guochunh@mail.sysu.edu.cn](mailto:guochunh@mail.sysu.edu.cn) (C. Guo).

<https://doi.org/10.1016/j.meegid.2018.11.002>

Received 27 July 2018; Received in revised form 11 September 2018; Accepted 1 November 2018

Available online 03 November 2018

1567-1348/© 2018 Elsevier B.V. All rights reserved.

poliovirus 1 (PV1) (Simonet and Gantzer, 2006) and echovirus 11 (E11) (Zhong et al., 2017). However, the mechanism that the inactivation of PRRSV by ClO<sub>2</sub> has not been reported.

In this study, we explored the antiviral effects of ClO<sub>2</sub> against PRRSV infection in vitro. We found that PRRSV infection and replication was effectively inhibited by ClO<sub>2</sub>. ClO<sub>2</sub> restrained PRRSV infection through blocking PRRSV binding to cells. Meanwhile, ClO<sub>2</sub> exerted extracellular antiviral activity against PRRSV as a result of the destruction of viral genome and proteins. Taken together, ClO<sub>2</sub> is of high value in clinical applications, which could be helpful for the antiviral therapies against PRRSV infection.

## 2. Materials and methods

### 2.1. Cells and viruses

Marc-145 cells (China Center for Type Culture Collection, China), an immortalized cell line derived from African green monkey kidney cells, were cultured in Dulbecco's modified Eagle's medium (DMEM) (Corning, USA) containing 10% fetal bovine serum (FBS) (PAN, Germany), which were permissive to PRRSV replication and commonly used in laboratories. Porcine alveolar macrophages (PAMs) were isolated from broncho-alveolar lavage fluid of three six-week-old PRRSV-negative pigs. Lungs were removed from thoracic cavity and washed the surface clean with phosphate buffer solution (PBS, Corning, USA). Lungs were lavaged with PBS and were gently massaged for three times. Cells were collected from bronchoalveolar lavage fluid (BALF) by centrifugation for 10 min at 1000 rpm, and then resuspended with RPMI-1640 medium (Gibco, USA) and centrifuged for 5 min at 1000 rpm. Finally, cells were frozen in 40% RPMI-1640 medium, 50% FBS, and 10% DMSO (Sigma, USA). PAMs were maintained in RPMI 1640 medium with 10% FBS at 37 °C in 5% CO<sub>2</sub>. No antibiotic was used in the culture during the experiments. All animal experiments were approved by the Institutional Animal Care and Use Committee of Sun Yat-sen University.

Three PRRSV strains, CHR6 (Classical North American type PRRSV strain) and Li11 (a highly pathogenic PRRSV isolate), were provided by Dr. Heng Wang from South China Agricultural University, and PRRSV-EGFP, a recombinant virus shows growth replication characteristics similar to those of the wild-type virus in the infected cells, was provided by Dr. Shuqi Xiao from Northwest A&F University (Wang et al., 2013). CHR6 and PRRSV-EGFP were used to infect Marc-145 cells, while PAMs were just infected with CHR6 in our research, because of the low infectivity of PRRSV-EGFP on PAMs. The three virus strains were propagated in Marc-145 cells and titrated as 50% tissue culture infective dose (TCID<sub>50</sub>).

### 2.2. Cytotoxicity assay

The cytotoxicity of ClO<sub>2</sub> was detected with the alamarBlue® assay (Invitrogen, USA) according to the manufacturer's instructions. Marc-145 cells (1 × 10<sup>4</sup>/well) and PAMs (1 × 10<sup>5</sup>/well) were seeded in 96-well plates respectively. Different concentrations of ClO<sub>2</sub> were added in DMEM and RPMI 1640 medium when cells grew to 60%–70% confluence. After incubation for 48 h in Marc-145 cells and PAMs, 10 µL of alamarBlue® was added to each well, and incubated for another 3 h. At last, the fluorescence value was detected using Multi-Mode Reader (Synergy2, BioTek, USA) at the absorbance of 570 nm.

### 2.3. Quantitative real-time reverse-transcription polymerase chain reaction (qRT-PCR)

In order to detect the relative expression of PRRSV ORF7 and cytokines, qRT-PCR should be used. Total RNA was extracted from cultured cells using TRIzol reagent (Magen, China). Reverse Transcription System (A3500, Promega, USA) were used for reverse transcription in

**Table 1**  
List of primers for RT-PCR.

Primer <sup>a</sup>	Sequence (5'–3') <sup>b</sup>
N-F	AAAACCAAGTCCAGAGGCAAG
N-R	CGGATCAGACGCACAGTATG
mGAPDH-F	TGACAACAGCCTCAAGATCG
mGAPDH-R	GTCTTCTGGGTGGCAGT GAT
mIL-6-F	AGAGGCACTGGCAGAAAAC
mIL-6-R	TGCAGGAAGTGGATCAGGAC
mTNF-α-F	TCTGTCTGCTGCACTTTGGAGTGA
mTNF-α-R	TTGAGGGTTTGTACAACATGGGC
mIFN-β-F	GCAATTGAATGGAAGGCTTGA
mIFN-β-R	CAGCGTCTCTCTCTGGAAC
ORF2a-F	ATGAAATGGGGTCTATGCAAG
ORF2a-R	TCACCATGAGTTCAAAAGAAAAGTT
ORF3-F	ATGGCTAATAGCTGTACATTC
ORF3-R	TCGCCGTGCGCACTG
ORF4-F	ATGGCTGCGTCTTTCTTTCTCT
ORF4-R	AAGCACTTCCCAACATCTTGAAC
ORF5-F	TGCTTCYAGATGAGTGAAA
ORF5-R	CAAAAGGTGCGAGAGCCCTA
ORF6-F	ATGGGTGCTCTCTAGATG
ORF6-R	TTTGGCATATTTAGCAAGG
ORF7-F	ATGCCAAATAACAACGGC
ORF7-R	TGCTGAGGGTGATGCTGT

<sup>a</sup> F, forward primer; R, reverse primer. The letter “m” indicates that it is for a monkey gene.

<sup>b</sup> Green monkey gene sequences and PRRSV gene sequences were downloaded from GenBank.

20 µL reaction volume following the manufacturer's instructions. The Reverse-transcription primers were Oligo (dT) 15 primer (C110A, Promega, USA) and Random primer (C118A, Promega, USA). Reverse-transcription products were amplified by a LightCycler 480 Real-Time PCR System (LC480, Roche, Switzerland) using 2 × RealStar Green Power Mixture (GenStar, China). The primers used for qRT-PCR are listed in Table 1. qRT-PCR reaction system was run under the following conditions: 95 °C for 10 min, then 95 °C for 15 s, 60 °C for 1 min and 72 °C for 30 s went through 40 cycles, finally 72 °C for 10 min. Data were normalized to GAPDH in each individual sample. The 2<sup>−ΔΔCt</sup> method was used to calculate relative expression changes. Relative expression (fold changes) was compared to mock infected cells.

### 2.4. Western blot

Six-well-plate cell samples (2 × 10<sup>6</sup>/well) were harvested in cell lysis buffer (Beyotime, China) containing PMSF (Beyotime, China). Processed samples was subjected to 12% sodium dodecyl sulfate-polyacrylamide gel electrophoresis (SDS-PAGE) and transferred onto a polyvinylidene difluoride (PVDF) membrane (Roche, USA). Then the membranes were blocked with 3% BSA (Ruishu, China) in TBST (20 mM Tris-HCl PH8.0, 150 mM NaCl, 0.05% Tween 20) for 1 h at 37 °C. After blocking they were incubated with an anti-PRRSV N protein monoclonal antibody (1:1000 dilution, Jeno Biotech, Inc., Republic of Korea), anti-glyceraldehyde phosphate dehydrogenase (GAPDH) antibody (1:1000 dilution, Cell Signaling Technology, USA) overnight at 4 °C. After washing four times with TBST buffer, membranes were incubated with anti-rabbit IgG, HRP-linked antibody or anti-rabbit IgG, HRP-linked antibody (1:1000 dilution, Cell Signaling Technology, USA) for 1 h at 37 °C. The antibody signals were exposed using a chemiluminescence (ECL) reagent (Fdbio Science, China).

### 2.5. Flow cytometry (FCM)

We used flow cytometry to detect the expression of PRRSV-EGFP, which indicated the viral replication. PRRSV-EGFP-infected cells were harvested and resuspended in PBS at a concentration of 1 × 10<sup>6</sup> cells/ml. Flow cytometry analyzed the ratio of GFP-positive cells and

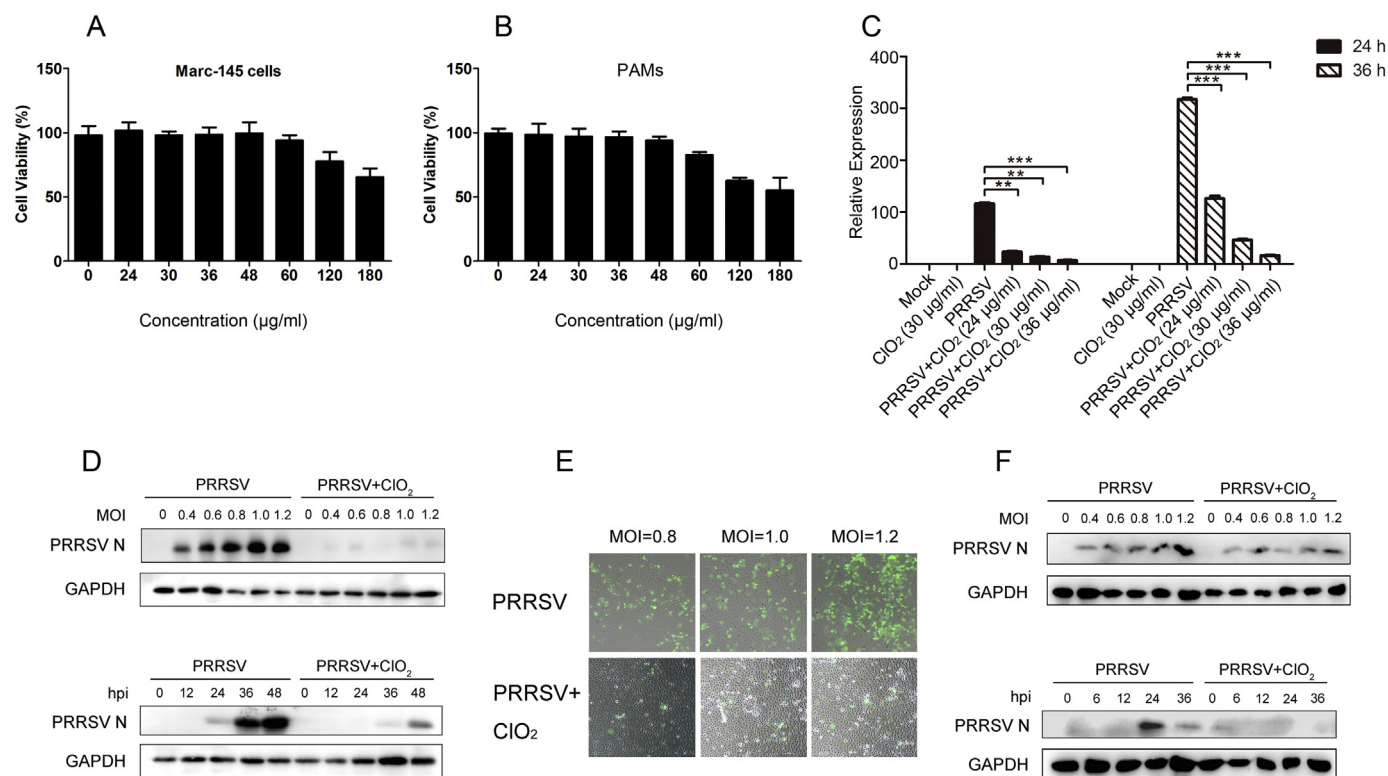


**Fig. 1.**  $\text{ClO}_2$  effectively suppresses the infection and replication of PRRSV both in Marc-145 cells and PAMs. (A) The cytotoxicity of  $\text{ClO}_2$  was measured by the alamarBlue assay. Marc-145 cells were treated with  $\text{ClO}_2$  at indicated concentrations for 48 h and cell viability assay was performed. (B) The cytotoxicity of  $\text{ClO}_2$  on PAMs was also measured using alamarBlue assay. (C) Marc-145 cells were mock infected or infected with PRRSV-EGFP (MOI = 0.6) in the presence of different concentrations of  $\text{ClO}_2$  (0, 24, 30, and 36  $\mu\text{g}/\text{mL}$ ) for 24 or 36 h. The expression of viral ORF7 (PRRSV N) was detected by qRT-PCR. (D and E) Marc-145 cells were infected with PRRSV-EGFP at different MOIs in the presence (30  $\mu\text{g}/\text{mL}$ ) or absence of  $\text{ClO}_2$ . N protein was determined by Western blot analysis (D) and GFP fluorescence of PRRSV was detected by immunofluorescence microscopy (E). (F) The same treatments were performed in porcine alveolar macrophages (PAMs), and Western blot was used to analyze the viral N protein at different MOIs and different infection periods. Data are representative of the results of three independent experiments (means  $\pm$  SE). Significant differences compared with control group are denoted by \* ( $P < .05$ ), \*\* ( $P < .01$ ) and \*\*\* ( $P < .001$ ).

fluorescence intensity, which represents the viral load. Typically, 10,000 labeled cells were acquired using a FACSCalibur (BD Bioscience, USA) and analyzed by FlowJo software.

## 2.6. Antiviral assay

Cells were seeded in six-well plates and grown to 70%–80% confluence. There were four approaches to analyze the antiviral effects of  $\text{ClO}_2$ . (I) Virucidal assay: PRRSV-EGFP (MOI = 0.6) was pre-incubated with different concentrations of  $\text{ClO}_2$  (0, 24, 30, and 36  $\mu\text{g}/\text{mL}$ ) for 2.5 h at 37 °C. The mixtures were then added to Marc-145 cells. After incubation for 4 h at 37 °C, the mixtures were removed. Cells were supplied with fresh DMEM containing 2% FBS and cultured for another 36 h. The supernatants were collected to detect viral titers. The cells were harvested for flow cytometry and immunoblotting analysis. (II) Pre-treatment: Cells were treated with different concentrations of  $\text{ClO}_2$  (0, 36 and 48  $\mu\text{g}/\text{mL}$ ) for 4 h, PRRSV-EGFP was then added and cultured for 36 h. (III) Co-treatment: Various concentrations of  $\text{ClO}_2$  (0, 36 and 48  $\mu\text{g}/\text{mL}$ ) were added to cells and cultured with PRRSV-EGFP together for 36 h. (IV) Post-treatment: Cells were inoculated with PRRSV-EGFP for 8 h, then the inoculum was removed and  $\text{ClO}_2$  (0, 36 and 48  $\mu\text{g}/\text{mL}$ ) was added to cells for another 36 h at 37 °C. In all above antiviral assays, the supernatants were collected to detect viral titers. In order to detect viral load and the expression of PRRSV capsid protein, cells were harvested for flow cytometry and immunoblotting analysis.

## 2.7. Viral attachment, entry and release assays

For attachment assay, cells were cooled for 2 h at 4 °C, and then

infected with PRRSV-EGFP (MOI = 0.6) in the presence of different concentrations of  $\text{ClO}_2$  (0, 24, 30, and 36  $\mu\text{g}/\text{mL}$ ) for 4 h at 4 °C. After rinsing with cold PBS for three times, cells were replenished with fresh DMEM containing 2% FBS for 36 h at 37 °C. The supernatants were harvested and titrated as TCID<sub>50</sub> and the cells were collected for flow cytometry and Western blot analysis so that we could determine the effects of  $\text{ClO}_2$  on viral attachment.

As for entry assay, cells were inoculated with PRRSV-EGFP (MOI = 0.6) for 4 h at 4 °C. After binding to cell surface, cells were washed with PBS three times and cultured at 37 °C for 6 h in the presence of various concentrations of  $\text{ClO}_2$  (0, 24, 30, and 36  $\mu\text{g}/\text{mL}$ ). When the temperature of culture medium switched to 37 °C,  $\text{ClO}_2$  was added to the cells at 0, 2, or 4 h (The moment that the temperature shift to 37 °C was regarded as 0 h). After incubation for total 6 h, cells were washed with PBS and incubated for another 36 h at 37 °C. Cells were collected to detect the viral burden by using flow cytometry and the supernatants were harvested and titrated as TCID<sub>50</sub> that implied virus infectivity.

For release assay, cells were incubated with PRRSV-EGFP (MOI = 0.6) for 36 h at 37 °C. After that, cells were rinsed with PBS three times and  $\text{ClO}_2$  at different concentrations was added to the cells for 6 h at 37 °C. At last, cells were collected for flow cytometry and Western blot analysis to detect the viral load and PRRSV N protein expression, respectively.

## 2.8. RT-PCR amplification of ORFs of viral genome

Viral RNA were abstracted using RaPure Viral RNA/DNA Kit (Magen, China). Titanium® One-Step RT-PCR Kit (TaKaRa, Japan) was

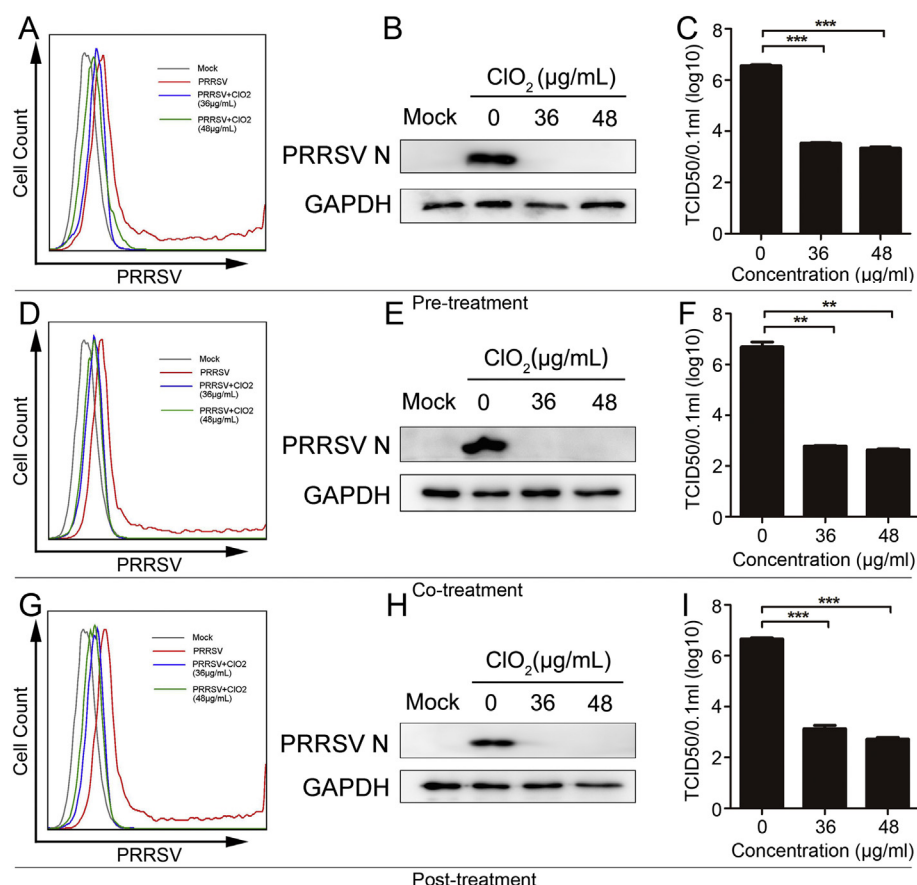


**Fig. 2.** Viral protein translation and PRRSV production were inhibited by ClO<sub>2</sub> treatment. (A–C) Marc-145 cells were pre-treated with different concentrations of ClO<sub>2</sub> (0, 36 and 48 μg/mL) for 4 h, then inoculated with PRRSV-EGFP at an MOI of 0.6 for 36 h, PRRSV-EGFP were detected by flow cytometry analysis (A). The protein levels of PRRSV N were determined by Western blot analysis (B). The supernatants were collected to detect viral titers (C). (D–F) Various concentrations of ClO<sub>2</sub> (0, 36 and 48 μg/mL) and PRRSV at an MOI of 0.6 were added to Marc-145 cells for 36 h. Cells were harvested for flow cytometry analysis (D) and immunoblotting analysis (E), and viral yields were detected in the supernatants (F). (G–I) Marc-145 cells were mock infected or infected with PRRSV-EGFP at an MOI of 0.6 for 8 h, and then ClO<sub>2</sub> (0, 36 and 48 μg/mL) was added. After incubation for another 36 h, PRRSV-EGFP was detected by flow cytometry (G), PRRSV N protein was determined by Western blot (H). Simultaneously, the supernatants were harvested to measure viral titers as TCID<sub>50</sub> (I). Data are representative of the results of three independent experiments (means ± SE). Significant differences compared with control group are denoted by \* ( $P < .05$ ), \*\* ( $P < .01$ ) and \*\*\* ( $P < .001$ ).

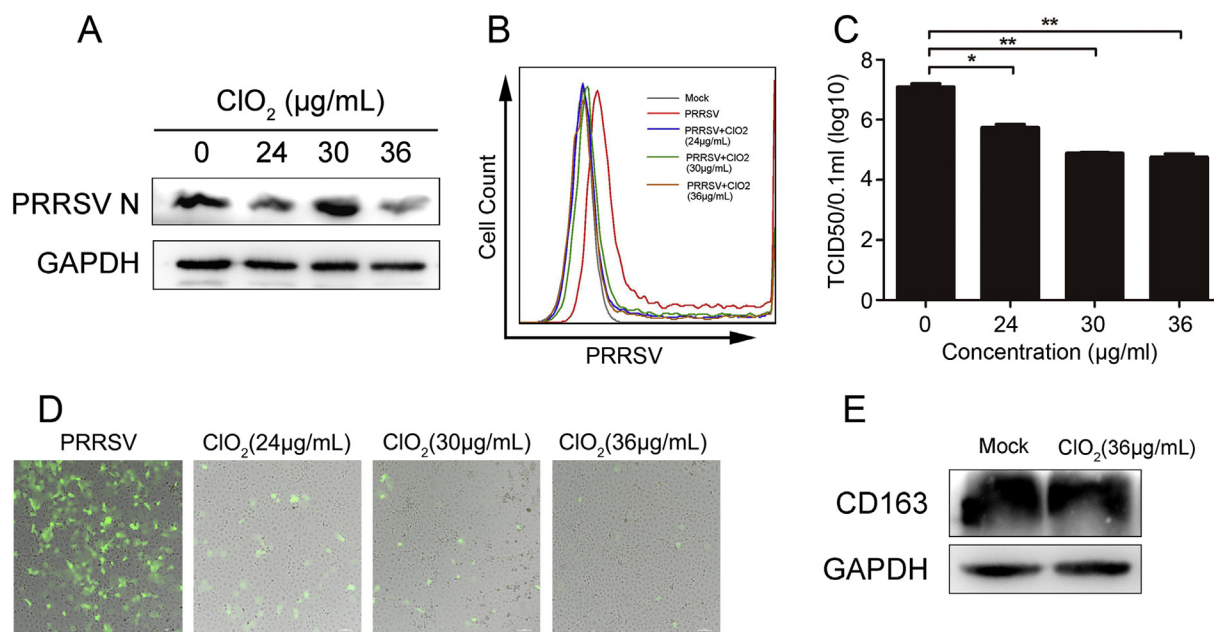


**Fig. 3.** Analysis of ClO<sub>2</sub> treatment effects on PRRSV attachment to Marc-145 cells. (A–D) Marc-145 cells were incubated with PRRSV-EGFP at an MOI of 0.6 in the presence of different concentrations of ClO<sub>2</sub> (0, 24, 30, and 36 μg/mL) for 4 h at 4 °C. After removing the unbound viral particles, cells were replenished with fresh DMEM and switched to 37 °C for 36 h. The expression of the viral N protein was detected by Western blot (A). Viral replication were determined by flow cytometry analysis (B) and viral production was measured and shown as TCID<sub>50</sub> (C). The fluorescence of PRRSV-EGFP was visual using immunofluorescence microscopy (Bar, 100 μm) (D). The expression of CD163 receptor in PAMs was detected by western blot in the absence and presence of ClO<sub>2</sub> (36 μg/mL) (E). Data are representative of the results of three independent experiments (means ± SE). Significant differences compared with the control group are denoted by \* ( $P < .05$ ), \*\* ( $P < .01$ ) and \*\*\* ( $P < .001$ ).



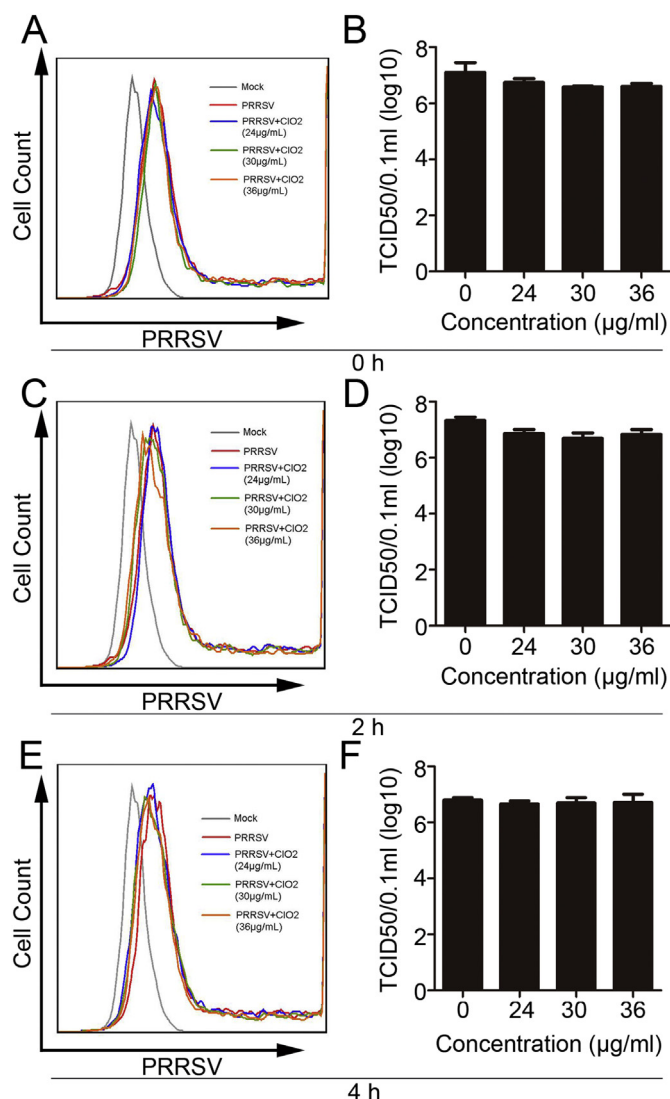


**Fig. 4.** Effects of  $\text{ClO}_2$  treatment on PRRSV entry. (A–F) Marc-145 cells were inoculated with PRRSV-EGFP at an MOI of 0.6 for 4 h at  $4^\circ\text{C}$ , unbound virus particles were removed,  $\text{ClO}_2$  (0, 24, 30, 36  $\mu\text{g/mL}$ ) was added accordingly at 0, 2, or 4 h after switching to  $37^\circ\text{C}$  in a time-of-addition manner. After incubation for total 6 h, cells were washed with PBS and incubated for another 36 h. At the indicated time 0 (A and B), 2 (C and D) or 4 h (E and F), cells were harvested. Positive cells infected with PRRSV-EGFP were tested by flow cytometry (A, C and E). Cultured supernatants were also collected to detect viral titers (B, D and F). Data are representative of the results of three independent experiments (means  $\pm$  SE). Significant differences that PRRSV infected cells in the presence and absence of  $\text{ClO}_2$  are denoted by \* ( $P < .05$ ), \*\* ( $P < .01$ ) and \*\*\* ( $P < .001$ ).

used for RNA reverse transcription. The primers of ORFs are listed in Table 1. The cycler program was consisted with  $94^\circ\text{C}$  for 4 min, then 30 cycles at  $94^\circ\text{C}$  for 30 s,  $55^\circ\text{C}$  for 30 s and  $72^\circ\text{C}$  for 1 min using 2  $\times$  SuperTaq PCR Mix with Loading Dye (GenStar, China).

## 2.9. Statistical analysis

All experiments were performed with at least three independent replicates. Student's *t*-test and one-way ANOVA were used to analyze the data. Statistical analysis was performed using SPSS 17.0 and GraphPad Prism 5.0.  $P < .05$  was considered to be significant.

## 3. Results

### 3.1. $\text{ClO}_2$ effectively suppresses the replication of PRRSV

To identify the antiviral activity of  $\text{ClO}_2$  against PRRSV, we first examined whether  $\text{ClO}_2$  can inhibit the replication of PRRSV on Marc-145 cells. Based on a cytotoxicity assay, concentrations of  $\text{ClO}_2$  that were non-cytotoxic were lower than 60  $\mu\text{g/mL}$  in Marc-145 cells after treatment for 48 h (Fig. 1A). PAMs cultured in medium containing 48  $\mu\text{g/mL}$   $\text{ClO}_2$  retained approximately relative viability of 100% compared with controls after treatment for 48 h (Fig. 1B). Marc-145 cells were mock infected or infected with PRRSV-EGFP (MOI = 0.6) in the presence of different concentrations of  $\text{ClO}_2$  (0, 24, 30, and 36  $\mu\text{g/mL}$ ) for 24 or 36 h. The mRNA relative expression of the viral ORF7 was reduced compared with the control group that PRRSV infected Marc-145 cells without  $\text{ClO}_2$ , which also exhibits its inhibiting effects in a dose-dependent manner (Fig. 1C). Next we investigated its effects on PRRSV infection, different MOIs of PRRSV-EGFP (at MOIs of 0.4, 0.6, 0.8, 1.0 or 1.2) were used to infect Marc-145 cells in the absence or presence of  $\text{ClO}_2$  (30  $\mu\text{g/mL}$ ). As shown in Fig. 1D and E,  $\text{ClO}_2$  significantly inhibited the replication of PRRSV regardless of different multiplicity of infections. Moreover,  $\text{ClO}_2$  suppressed PRRSV infection in a time-dependent manner when we evaluated its effects on PRRSV (MOI = 0.6) at 12, 24, 36, and 48 h post-infection (hpi) (Fig. 1D). To investigate whether the same antiviral effects can be observed on PAMs, which are susceptible cells of PRRSV in vivo, we did the same experiments with CHR6 strain in PAMs. Consistent with the findings obtained with Marc-145 cells,  $\text{ClO}_2$  showed a potent antiviral activity against PRRSV in dose- and time-dependent manners (Fig. 1F).

### 3.2. Viral protein translation and PRRSV production were inhibited by $\text{ClO}_2$ treatment

To further demonstrate that  $\text{ClO}_2$  has great ability to influence the infection of PRRSV, the effects of treatment with  $\text{ClO}_2$  were analyzed with three different approaches as described in the materials and methods. Compared with control group, the virus titers and viral load were significantly decreased following the pre- or co-treatment of  $\text{ClO}_2$  in Marc-145 cells infected with PRRSV (Fig. 2A, C, D and F). The N protein of PRRSV were also reduced by the pre- or co-treatment of  $\text{ClO}_2$  (Fig. 2B and E). Consistent with the findings obtained with pre-treatment and co-treatment methods, the expression of PRRSV and viral titers were decreased by  $\text{ClO}_2$  when administered with post-treatment in Marc-145 cells (Fig. 2G–I). Taken together,  $\text{ClO}_2$  exerts the efficiency on the suppression of PRRSV infection in Marc-145 cells.

### 3.3. $\text{ClO}_2$ blocks PRRSV binding to cell surface

We have identified that  $\text{ClO}_2$  can inhibit the replication of PRRSV, but the underlying molecular mechanism that the antiviral activity of  $\text{ClO}_2$  against PRRSV remains unknown. Virus invasion mainly has 4 processes: binding, entry, replication and release. To characterize which stage of the viral life cycle is interrupted by  $\text{ClO}_2$ , an attachment assay was initially used to test whether  $\text{ClO}_2$  can block PRRSV binding to Marc-145 cells. PRRSV infected Marc-145 cells with absence of  $\text{ClO}_2$  regarded as control group. As shown in Fig. 3A,  $\text{ClO}_2$  significantly reduced the N protein level of PRRSV during the period of viral attachment. The number of PRRSV-EGFP-infected cells, fluorescent yield and viral titer were all decreased in  $\text{ClO}_2$ -treated cells as well (Fig. 3B, C, and D). To identify whether  $\text{ClO}_2$  could destroy the cell receptors, we also detected the expression of CD163 receptor in PAMs, which was the most important receptor for PRRSV infection. As shown in Fig. 3E,  $\text{ClO}_2$  had no effect on the expression of CD163 receptor. These data suggest that  $\text{ClO}_2$  is able to observably reduce the virus particles attaching to the receptors of cell surface.

Next we investigated whether  $\text{ClO}_2$  can block viral entry. We added

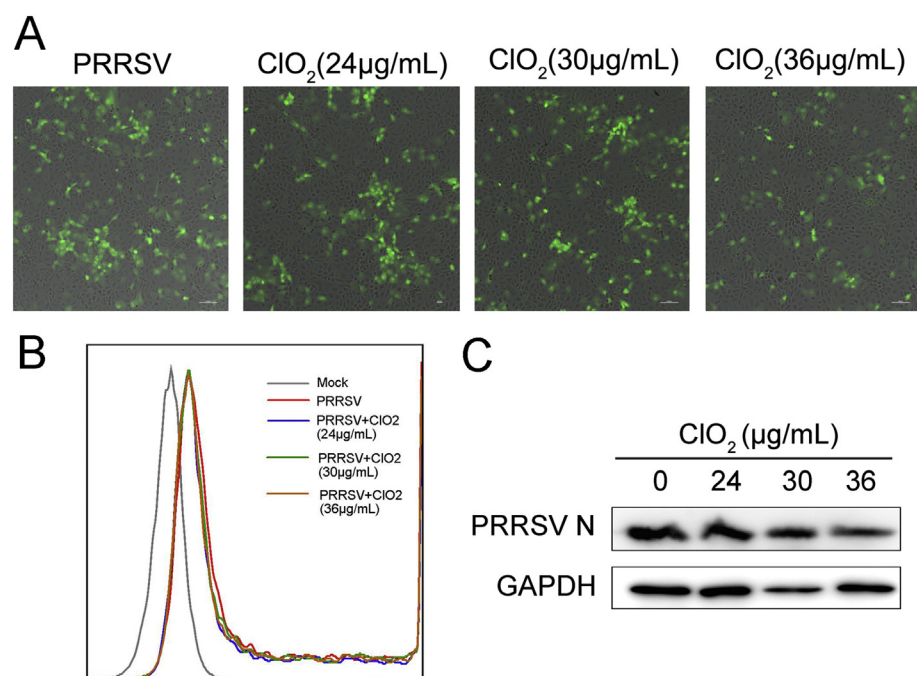


**Fig. 5.** ClO<sub>2</sub> has no influence on the release of PRRSV. (A–C) Cells were incubated with PRRSV-EGFP at an MOI of 0.6 for 36 h at 37 °C. After that, ClO<sub>2</sub> at different concentrations (0, 24, 30, and 36 µg/mL) was added to the cells for 6 h. Cells were harvested to identify viral load using immunofluorescence analysis (Bar, 100 µm) (A) and flow cytometry analysis (B) respectively. PRRSV N protein levels were detected by Western blot (C). Data are representative of the results of three independent experiments (means ± SE). Significant differences compared with control group are denoted by \* ( $P < .05$ ), \*\* ( $P < .01$ ) and \*\*\* ( $P < .001$ ).

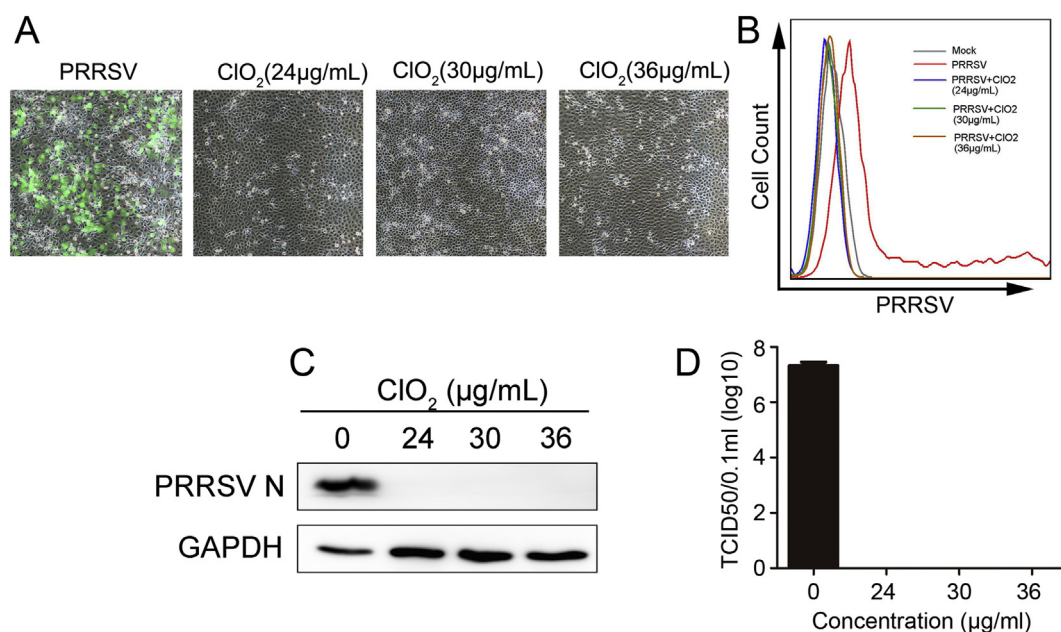


**Fig. 6.** ClO<sub>2</sub> displays extracellular virucidal activity against PRRSV. (A–D) PRRSV-EGFP was pre-incubated with different concentrations of ClO<sub>2</sub> (0, 24, 30, and 36 µg/mL) for 2.5 h at 37 °C. The mixtures was added to Marc-145 cells for 4 h. Afterwards, cells were supplied with fresh DMEM and cultured for another 36 h. PRRSV-EGFP were detected by immunofluorescence microscopy (Bar, 100 µm) (A). Flow cytometry was used to detect PRRSV-EGFP positive cells (B) and the expression of viral N protein was determined by Western blot (C). The virus titers (TCID<sub>50</sub>) were also analyzed (D). The data represent the means ± SE from three independent experiments (\*,  $P < .05$ ; \*\*,  $P < .01$ ; \*\*\*,  $P < .001$ ; ND means non-detectable).

ClO<sub>2</sub> to the infected Marc-145 cells at the entry stage of the viral life cycle. As shown in Fig. 4, there was no significant change in viral titer and viral fluorescence intensity when ClO<sub>2</sub> was added at 0 (Fig. 4A and B), 2 (Fig. 4C and D) or 4 h (Fig. 4E and F) after the medium temperature shifting to 37 °C, indicating that ClO<sub>2</sub> has little effect during the period of viral entry.

Finally, we examined the effects of ClO<sub>2</sub> on the release process of PRRSV life cycle in Marc-145 cells. As shown in Fig. 5, there was no effect on the GFP fluorescence of PRRSV (Fig. 5A and B). ClO<sub>2</sub> could not reduce the N protein of PRRSV during the stage of viral release (Fig. 5C). Taken together, ClO<sub>2</sub> blocks PRRSV binding to cell membrane

rather than the processes of entry and release in Marc-145 cells.

#### 3.4. ClO<sub>2</sub> displays extracellular antiviral activity against PRRSV

ClO<sub>2</sub> acts as a new broad spectrum high effect disinfectant, which has strong inactivated effect on viruses, bacteria, fungi and mycotic spores (Sigstam et al., 2014). To investigate the direct inactivation effect of ClO<sub>2</sub> against PRRSV, a virucidal assay described in the materials and methods was performed on Marc-145 cells. PRRSV pre-incubated with absence of ClO<sub>2</sub> regarded as control group. We could not find any viral fluorescence in PRRSV-infected cells with ClO<sub>2</sub> treatment using

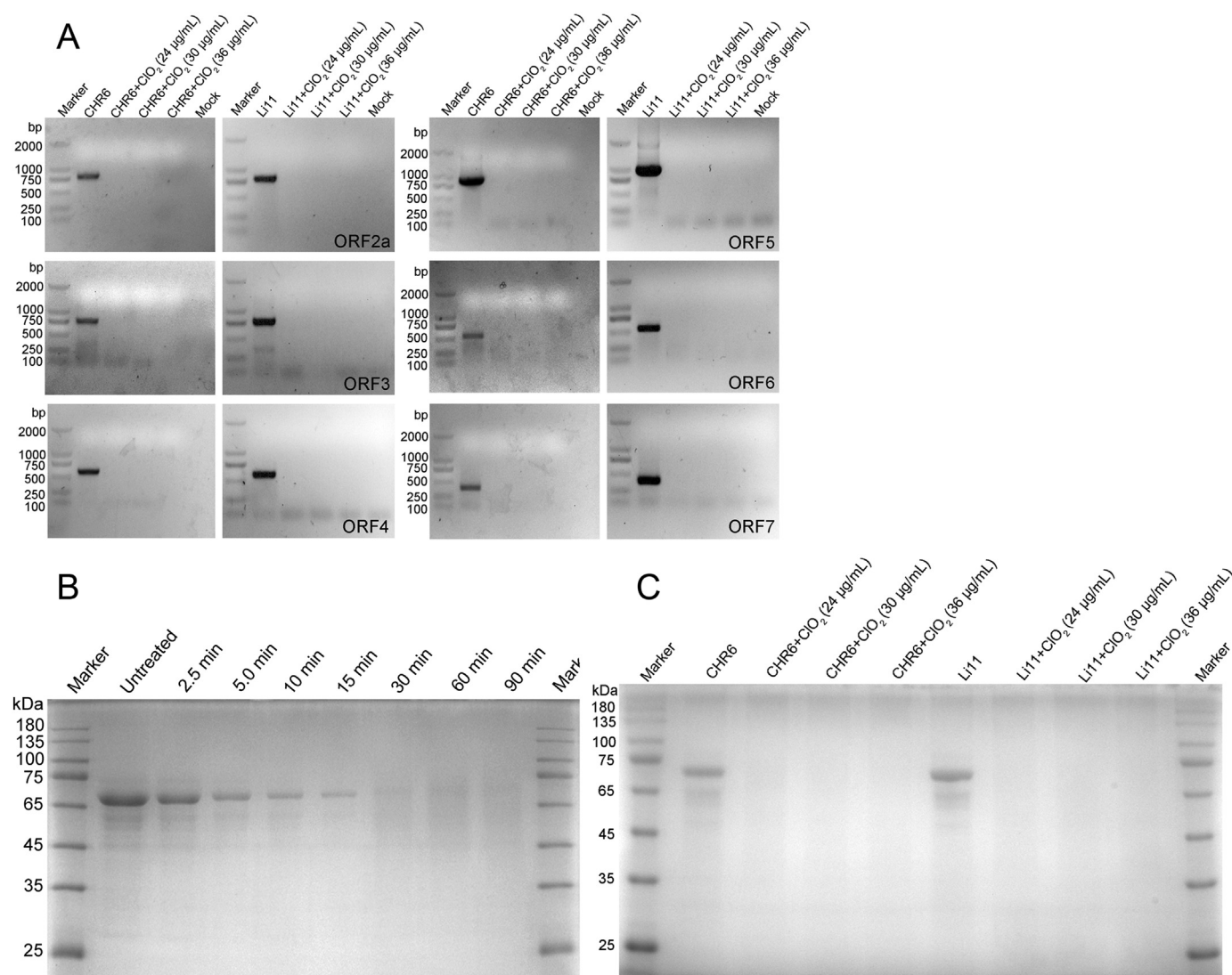


**Fig. 7.** The inactivation of PRRSV by ClO<sub>2</sub> is mainly driven by genome and protein damage. (A–C) CHR6 or Li11 were incubated with different concentrations of ClO<sub>2</sub> (0, 24, 30, and 36 µg/mL) for 2 h. ORF2a (771 bp), ORF3 (762 bp), ORF4 (564 bp), ORF5 (914 bp), ORF6 (522 bp), and ORF7 (369 bp) of CHR6 and Li11 were amplified using RT-PCR (A). The degradation process of CHR6 proteins at the indicated times after treatment with ClO<sub>2</sub> was examined (B). Meanwhile, the mixtures of CHR6, Li11 and ClO<sub>2</sub> were subjected to SDS-PAGE analysis (C). Data are representative of the results of three independent experiments.

fluorescence microscope (Fig. 6A). On the contrary, there was full of GFP fluorescence which represents viral burden in visual field following the treatment of PRRSV only (Fig. 6A). Compared to PRRSV control group, the amount of GFP fluorescence were significantly reduced by the treatment of ClO<sub>2</sub> (Fig. 6B). Consistently, N protein and viral titers were undetectable in cells treated with ClO<sub>2</sub> (Fig. 6C and D). All these data indicate that PRRSV is completely inactivated by the treatment of ClO<sub>2</sub> in Marc-145 cells.

### 3.5. The inactivation of PRRSV by ClO<sub>2</sub> is mainly driven by genome and protein damage

We demonstrated that ClO<sub>2</sub> inhibits PRRSV replication, but how it works is still unknown. Nucleocapsid is the basic structure of the virus, which contains nucleic acids and proteins (Doan and Dokland, 2003; Dokland, 2010). To investigate whether ClO<sub>2</sub> destroys the structure of proteins and genome, ClO<sub>2</sub> at the indicated concentrations (0, 24, 30, 36 µg/mL) was incubated with classical strain CHR6 or highly pathogenic strain Li11 for 2 h at 37 °C, and then the mixtures were harvested for viral proteins and ORFs analysis by SDS-PAGE (Coomassie brilliant blue staining) and RT-PCR respectively. As shown in Fig. 7A, RNA

fragments of ORF2a, ORF3, ORF4, ORF5, ORF6, ORF7 were all undetectable when CHR6 and Li11 were treated with ClO<sub>2</sub> (0, 24, 30, 36 µg/mL), suggesting that ClO<sub>2</sub> destroys the structure of viral genome. Next, we explored the dynamic change of viral proteins at the indicated times after treatment with ClO<sub>2</sub>. The degradable functions of ClO<sub>2</sub> on CHR6 worked in a time-dependent manner. At the time of 5 min, viral proteins started to break down and PRRSV was absolutely degraded at 30 min (Fig. 7B). Moreover, the structural proteins were degraded both in CHR6 and Li11 (Fig. 7C). These data demonstrate that ClO<sub>2</sub> can degrade the structural proteins of PRRSV and destroy viral genome resulting in the inactivation of PRRSV.

### 3.6. ClO<sub>2</sub> decreases the level of inflammatory cytokines induced by PRRSV

PRRSV causes acute interstitial pneumonia after infection because of the accumulation of a large number of inflammatory factors (Thanawongnuwech et al., 2004). To investigate the effect of ClO<sub>2</sub> on the expression of cytokines in Marc-145 cells, Marc-145 cells were mock infected or infected with CHR6 (MOI = 0.1) in the presence of different concentrations of ClO<sub>2</sub> (0, 24, 30, and 36 µg/mL) for 24 or 36 h. qRT-PCR was conducted to evaluate the expression of pro-



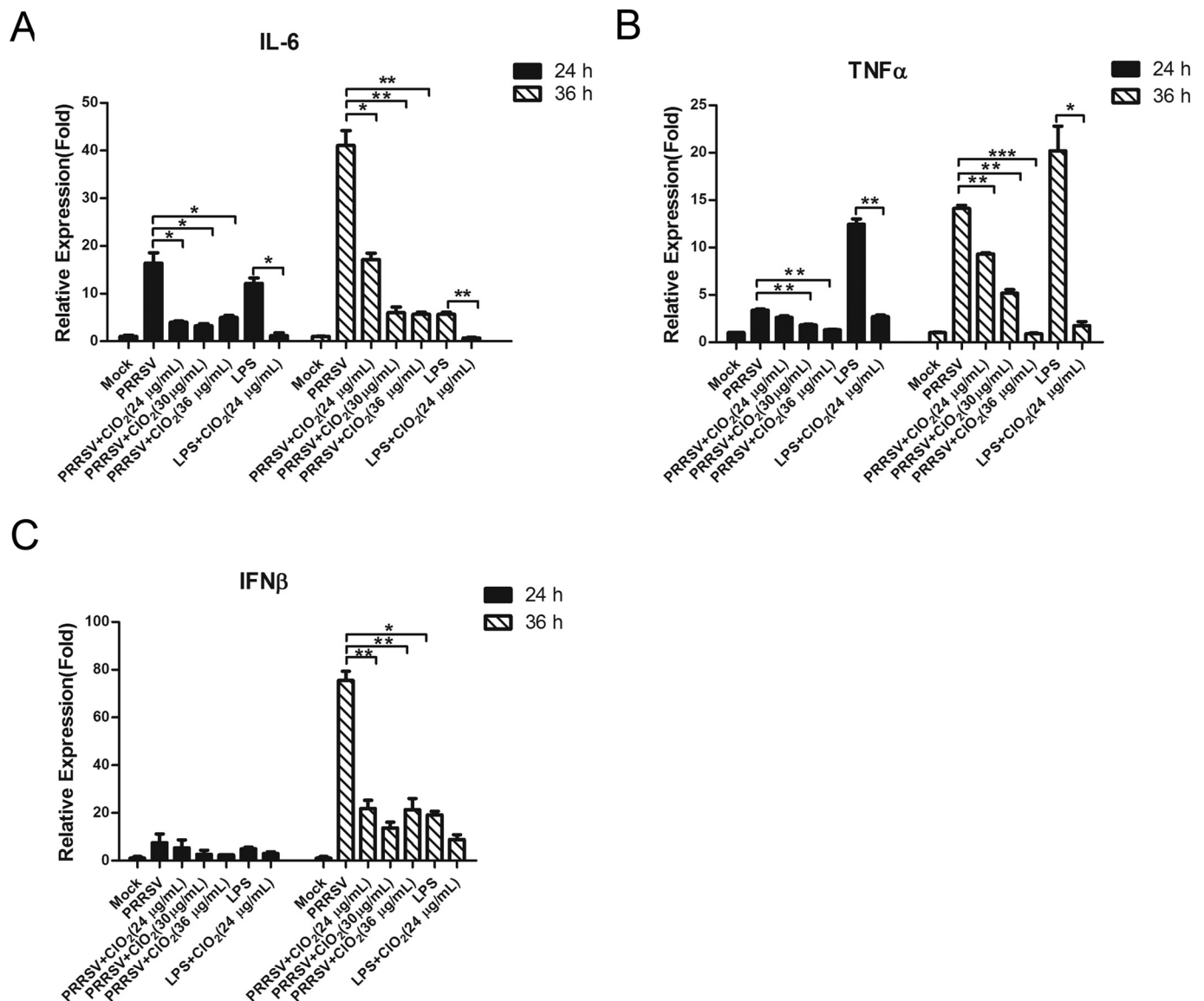


**Fig. 8.** Expression of cytokines in Marc-145 cells treated with ClO<sub>2</sub>. (A–C) Marc-145 cells were mock infected or infected with CHR6 (MOI = 0.1) in the presence of different concentrations of ClO<sub>2</sub> (0, 24, 30, and 36 μg/mL) for 24 or 36 h. The expression of pro-inflammatory cytokines IL-6 (A), TNF-α (B), and IFN-β (C) were analyzed using qRT-PCR at 24 and 36 hpi. LPS was served as positive control. Relative expression (fold) in comparison with mock infected cells (set up as 1) is shown. Data are the results of three independent experiments (means ± SE). Significant differences between PRRSV infected cells and those treated with ClO<sub>2</sub> are denoted by \* ( $P < .05$ ), \*\* ( $P < .01$ ) and \*\*\* ( $P < .001$ ).

inflammatory cytokines interleukin-6 (IL-6), tumor necrosis factor-α (TNF-α) and IFN-β. LPS was served as positive control. As shown in Fig. 8A and B, there was a significant decrease on the expression of IL-6 and TNF-α in cells treated with ClO<sub>2</sub> and PRRSV compared to those treated with PRRSV alone, and this phenomenon caused by ClO<sub>2</sub> was in a dose-dependent manner at 24 and 36 hpi. Consistently, the expression of IFN-β was significantly reduced by ClO<sub>2</sub> in cells at 36 hpi (Fig. 8C). Taken together, these data suggest that ClO<sub>2</sub> reduces the mRNA level of pro-inflammatory cytokines induced by PRRSV, maintaining a steady state for the growth of cells.

#### 4. Discussion

PRRSV is one of the most economically important disease of pigs worldwide. PRRS is initially reported in North America in late 1980s (Neumann et al., 2005). PRRSV has quickly spread many countries and has become a major problem in preventing swine diseases in China (Murtaugh et al., 2010). Besides, its high variation and persistent

infection make it difficult to control (Murtaugh et al., 2010; Stadejek et al., 2013). To prevent PRRSV infection, many methods are applied to interrupt the different stages of viral life cycle. Current PRRS vaccines such as MLVs fail to effectively prevent and control this disease (Kimman et al., 2009; Murtaugh and Genzow, 2011). Some novel vaccines with specific adjuvants are emerged in recent years, but they provide little protection (Du et al., 2017a). Some drugs, for example herbal extracts, chemical compounds, siRNA, microRNA and neutralizing antibodies have been verified that they can inhibit the replication of PRRSV in vitro (Du et al., 2017a). However, it is not sure whether they still maintain the antiviral activity but do no harm to animal bodies in vivo. Therefore, these agents are far from being ready for practical use in anti-PRRSV therapy. Despite the sustained effort, the prevention and treatment of PRRSV are still unavailable. In this study, we identified that ClO<sub>2</sub> has a strong inhibitory effect against PRRSV infection and replication with no cytotoxicity in both Marc-145 cells and PAMs (Fig. 1).

In antiviral assay, ClO<sub>2</sub> strongly inhibited PRRSV replication when



Marc-145 cells were infected with PRRSV-EGFP and pre-, co-, or post-treated with ClO<sub>2</sub> for 36 h (Fig. 2), indicating that ClO<sub>2</sub> might directly affect virus by impairing RNA and protein synthesis. PRRSV enters host cells through receptor-mediated viral entry and endocytosis, CD163 has been determined to be an essential receptor for viral internalization (Shi et al., 2015; Zhang and Yoo, 2015). The first step of viral invasion needs the attachment of PRRSV towards cellular receptor. Previous studies have demonstrated that GP2a and GP4 are viral attachment proteins interacting with CD163, suggesting that viral GPs play an important role in host-cell binding even entry (Wang et al., 2011; Welch and Calvert, 2010). Then we carried attachment, entry and release assays at multiple stages of the viral life cycle, we found that ClO<sub>2</sub> inhibited the process of PRRSV binding to Marc-145 cells (Fig. 3). Meanwhile our results demonstrated that ClO<sub>2</sub> could inactivate virus through breaking down the genome and structural proteins of PRRSV (Figs. 6 and 7). Presumably, the underlying mechanisms may be the destruction of GPs so that the interaction between PRRSV and cell receptors is possibly blocked and the life cycle of PRRSV is terminated by ClO<sub>2</sub>. On the contrary, there is no influence on viral entry and release when treated with ClO<sub>2</sub> (Figs. 4 and 5). Thus ClO<sub>2</sub> mainly blocked attachment stage of virus life cycle, indicating that PRRSV inactivation by ClO<sub>2</sub> leads to the inability of the virus to bind to its host. However, whether ClO<sub>2</sub> can alter the structure of cell receptors is still unclear and accordingly would be our next issue to be addressed in future.

PRRSV infection induces the release of pro-inflammatory factors, such as IL-1, IL-6, TNF- $\alpha$ , which may contribute to the pathogenesis and inflammation response (Hao et al., 2015; Thanawongnuwech et al., 2004). Persistent and increased production may lead to cell apoptosis. Our study demonstrated that ClO<sub>2</sub> inhibited inflammatory response in PRRSV-infected Marc-145 cells via decreasing the mRNA levels of the pro-inflammatory cytokines (Fig. 8). ClO<sub>2</sub> moderates PRRSV-induced inflammatory responses associated with viral replication and promotes host resistance against PRRSV infection. Many signal transduction pathways can modulate pro-inflammatory gene expression, such as NF- $\kappa$ B, MAPK and so on. More studies are required to verify whether ClO<sub>2</sub> has the influence on signal transduction pathways.

In conclusion, our study demonstrates that ClO<sub>2</sub>, the purity is 99%, inhibits the infection and replication of PRRSV by targeting attachment process in the viral life cycle. ClO<sub>2</sub> has strong inactivated effects on PRRSV through degrading viral genome and proteins. It is possible that ClO<sub>2</sub> can serve as a potential agent against PRRSV infection.

## Acknowledgements

This work was supported by National Natural Science Foundation of China (31601917), Natural Science Foundation of Guangdong Province (2014A030312011), and Science and Technology Planning Project of Guangzhou (201804020039).

## Conflicts of interests

The authors declare that they have no conflict of interests.

## References

Chen, Y.S., Vaughn, J.M., 1990. Inactivation of human and simian rotaviruses by chlorine dioxide. *Appl. Environ. Microbiol.* 56, 1363–1366.

Doan, D.N., Dokland, T., 2003. Structure of the nucleocapsid protein of porcine reproductive and respiratory syndrome virus. *Structure* 11, 1445–1451. <https://doi.org/10.1016/j.str.2003.09.018>.

Dodd, M.C., 2012. Potential impacts of disinfection processes on elimination and deactivation of antibiotic resistance genes during water and wastewater treatment. *J. Environ. Monit.* 14, 1754–1771. <https://doi.org/10.1039/c2em00006g>.

Dokland, T., 2010. The structural biology of PRRSV. *Virus Res.* 154, 86–97. <https://doi.org/10.1016/j.virusres.2010.07.029>.

Du, T., Nan, Y., Xiao, S., Zhao, Q., Zhou, E.M., 2017a. Antiviral strategies against PRRSV infection. *Trends Microbiol.* 25, 968–979. <https://doi.org/10.1016/j.tim.2017.06.001>.

Du, T., Shi, Y., Xiao, S., Li, N., Zhao, Q., Zhang, A., Nan, Y., Mu, Y., Sun, Y., Wu, C., Zhang,

H., Zhou, E.M., 2017b. Curcumin is a promising inhibitor of genotype 2 porcine reproductive and respiratory syndrome virus infection. *BMC Vet. Res.* 13 (298). <https://doi.org/10.1186/s12917-017-1218-x>.

Fang, Y., Snijder, E.J., 2010. The PRRSV replicase: exploring the multifunctionality of an intriguing set of nonstructural proteins. *Virus Res.* 154, 61–76. <https://doi.org/10.1016/j.virusres.2010.07.030>.

Gomez-Laguna, J., Salguero, F.J., Pallares, F.J., Carrasco, L., 2013. Immunopathogenesis of porcine reproductive and respiratory syndrome in the respiratory tract of pigs. *Vet. J.* 195, 148–155. <https://doi.org/10.1016/j.tvjl.2012.11.012>.

Guo, Z., Chen, X.X., Li, R., Qiao, S., Zhang, G., 2018. The prevalent status and genetic diversity of porcine reproductive and respiratory syndrome virus in China: a molecular epidemiological perspective. *Virology* 15 (2). <https://doi.org/10.1186/s12985-017-0910-6>.

Hao, H.P., Wen, L.B., Li, J.R., Wang, Y., Ni, B., Wang, R., Wang, X., Sun, M.X., Fan, H.J., Mao, X., 2015. LiCl inhibits PRRSV infection by enhancing Wnt/beta-catenin pathway and suppressing inflammatory responses. *Antivir. Res.* 117, 99–109. <https://doi.org/10.1016/j.antiviral.2015.02.010>.

Jin, M., Shan, J., Chen, Z., Guo, X., Shen, Z., Qiu, Z., Xue, B., Wang, Y., Zhu, D., Wang, X., Li, J., 2013. Chlorine dioxide inactivation of enterovirus 71 in water and its impact on genomic targets. *Environ. Sci. Technol.* 47, 4590–4597. <https://doi.org/10.1021/es305282g>.

Kimman, T.G., Cornelissen, L.A., Moormann, R.J., Rebel, J.M., Stockhofe-Zurwieden, N., 2009. Challenges for porcine reproductive and respiratory syndrome virus (PRRSV) vaccinology. *Vaccine* 27, 3704–3718. <https://doi.org/10.1016/j.vaccine.2009.04.022>.

King, A.M.Q., Lefkowitz, E.J., Mushegian, A.R., Adams, M.J., Dutilh, B.E., Gorbalenya, A.E., Harrach, B., Harrison, R.L., Junglen, S., Knowles, N.J., Kropinski, A.M., Krupovic, M., Kuhn, J.H., Nibert, M.L., Rubino, L., Sabanadzovic, S., Sanfacon, H., Siddell, S.G., Simmonds, P., Varsani, A., Zerbini, F.M., Davison, A.J., 2018. Changes to taxonomy and the International Code of Virus Classification and Nomenclature ratified by the International Committee on Taxonomy of Viruses (2018). *Arch. Virol.* 163, 2601–2631. <https://doi.org/10.1007/s00705-018-3847-1>.

Li, Y., Tas, A., Sun, Z., Snijder, E.J., Fang, Y., 2015. Proteolytic processing of the porcine reproductive and respiratory syndrome virus replicase. *Virus Res.* 202, 48–59. <https://doi.org/10.1016/j.virusres.2014.12.027>.

Lim, M.Y., Kim, J.M., Ko, G., 2010. Disinfection kinetics of murine norovirus using chlorine and chlorine dioxide. *Water Res.* 44, 3243–3251. <https://doi.org/10.1016/j.watres.2010.03.003>.

Liu, F., Du, Y., Feng, W.H., 2017. New perspective of host microRNAs in the control of PRRSV infection. *Vet. Microbiol.* 209, 48–56. <https://doi.org/10.1016/j.vetmic.2017.01.004>.

Lunney, J.K., Benfield, D.A., Rowland, R.R., 2010. Porcine reproductive and respiratory syndrome virus: an update on an emerging and re-emerging viral disease of swine. *Virus Res.* 154, 1–6. <https://doi.org/10.1016/j.virusres.2010.10.009>.

Montazeri, N., Manuel, C., Moorman, E., Khawitwada, J.R., Williams, L.L., Jaykus, L.A., 2017. Virucidal activity of fogged chlorine dioxide- and hydrogen peroxide-based disinfectants against human norovirus and its surrogate, feline calicivirus, on hard-to-reach surfaces. *Front. Microbiol.* 8 (1031). <https://doi.org/10.3389/fmicb.2017.01031>.

Murtaugh, M.P., Genzow, M., 2011. Immunological solutions for treatment and prevention of porcine reproductive and respiratory syndrome (PRRS). *Vaccine* 29, 8192–8204. <https://doi.org/10.1016/j.vaccine.2011.09.013>.

Murtaugh, M.P., Stadejek, T., Abraham, J.E., Lam, T.T., Leung, F.C., 2010. The ever-expanding diversity of porcine reproductive and respiratory syndrome virus. *Virus Res.* 154, 18–30. <https://doi.org/10.1016/j.virusres.2010.08.015>.

Neumann, E.J., Kliebenstein, J.B., Johnson, C.D., Mabry, J.W., Bush, E.J., Seitzinger, A.H., Green, A.L., Zimmerman, J.J., 2005. Assessment of the economic impact of porcine reproductive and respiratory syndrome on swine production in the United States. *J. Am. Vet. Med. Assoc.* 227, 385–392. <https://doi.org/10.2460/javma.2005.227.385>.

Shi, C., Liu, Y., Ding, Y., Zhang, Y., Zhang, J., 2015. PRRSV receptors and their roles in virus infection. *Arch. Microbiol.* 197, 503–512. <https://doi.org/10.1007/s00203-015-1088-1>.

Sigstam, T., Rohatschek, A., Zhong, Q., Brennecke, M., Kohn, T., 2014. On the cause of the tailing phenomenon during virus disinfection by chlorine dioxide. *Water Res.* 48, 82–89. <https://doi.org/10.1016/j.watres.2013.09.023>.

Simonet, J., Gantzer, C., 2006. Degradation of the Poliovirus 1 genome by chlorine dioxide. *J. Appl. Microbiol.* 100, 862–870. <https://doi.org/10.1111/j.1365-2672.2005.02850.x>.

Stadejek, T., Stankevicius, A., Murtaugh, M.P., Oleksiewicz, M.B., 2013. Molecular evolution of PRRSV in Europe: current state of play. *Vet. Microbiol.* 165, 21–28. <https://doi.org/10.1016/j.vetmic.2013.02.029>.

Thanawongnuwech, R., Thacker, B., Halbur, P., Thacker, E.L., 2004. Increased production of proinflammatory cytokines following infection with porcine reproductive and respiratory syndrome virus and mycoplasma hyopneumoniae. *Clin. Diagn. Lab. Immunol.* 11, 901–908. <https://doi.org/10.1128/CDLI.11.5.901-908.2004>.

Vu, H.L.X., Pattnaik, A.K., Osorio, F.A., 2017. Strategies to broaden the cross-protective efficacy of vaccines against porcine reproductive and respiratory syndrome virus. *Vet. Microbiol.* 206, 29–34. <https://doi.org/10.1016/j.vetmic.2016.09.014>.

Wang, L., Zhang, H., Suo, X., Zheng, S., Feng, W.H., 2011. Increase of CD163 but not sialoadhesin on cultured peripheral blood monocytes is coordinated with enhanced susceptibility to porcine reproductive and respiratory syndrome virus infection. *Vet. Immunol. Immunopathol.* 141, 209–220. <https://doi.org/10.1016/j.vetimm.2011.03.001>.

Wang, C.B., Huang, B.C., Kong, N., Li, Q.Y., Ma, Y.P., Li, Z.J., Gao, J.M., Zhang, C., Wang, X.P., Liang, C., Dang, L., Xiao, S.Q., Mu, Y., Zhao, Q., Sun, Y.N., Almazan, F.,

- Enjuanes, L., Zhou, E.M., 2013. A novel porcine reproductive and respiratory syndrome virus vector system that stably expresses enhanced green fluorescent protein as a separate transcription unit. *Vet. Res.* 44, 104. <https://doi.org/10.1186/1297-9716-44-104>.
- Welch, S.K., Calvert, J.G., 2010. A brief review of CD163 and its role in PRRSV infection. *Virus Res.* 154, 98–103. <https://doi.org/10.1016/j.virusres.2010.07.018>.
- Wootton, Sarah K., Nelson, Eric A., Yoo, D., 1998. Antigenic structure of the nucleocapsid protein of porcine reproductive and respiratory syndrome virus. *Clin. Diagn. Lab. Immunol.* 5, 773–779.
- Yang, Q., Gao, L., Si, J., Sun, Y., Liu, J., Cao, L., Feng, W.H., 2013. Inhibition of porcine reproductive and respiratory syndrome virus replication by flavaspidic acid AB. *Antivir. Res.* 97, 66–73. <https://doi.org/10.1016/j.antiviral.2012.11.004>.
- Yun, S.I., Lee, Y.M., 2013. Overview: Replication of porcine reproductive and respiratory syndrome virus. *J. Microbiol.* 51, 711–723. <https://doi.org/10.1007/s12275-013-3431-z>.
- Zhang, Q., Yoo, D., 2015. PRRS virus receptors and their role for pathogenesis. *Vet. Microbiol.* 177, 229–241. <https://doi.org/10.1016/j.vetmic.2015.04.002>.
- Zhong, Q., Carratala, A., Shim, H., Bachmann, V., Jensen, J.D., Kohn, T., 2017. Resistance of echovirus 11 to ClO<sub>2</sub> is associated with enhanced host receptor use, altered entry routes, and high fitness. *Environ. Sci. Technol.* 51, 10746–10755. <https://doi.org/10.1021/acs.est.7b03288>.